Inside polyomavirus at 25-Å resolution

James P. Griffith*, Diana L. Griffith*, Ivan Rayment*†, William T. Murakami‡ & Donald L. D. Caspar*§

* Rosenstiel Basic Medical Sciences Research Center, Brandeis University, Waltham, Massachusetts 02254, USA
‡ Graduate Department of Biochemistry, Brandeis University Waltham, Massachusetts 02254, USA

EMPTY capsids and complete virions of polyomavirus crystallize isomorphously[1]. Here we use difference Fourier analysis of X-ray diffraction data at 25-Å resolution from these crystals to obtain an electron-density map of the inside of the virion. The polyomavirus capsid is built from 72 pentamers of VP1 that form three different types of connections in the $T=7d$ icosahedral surface lattice[2]. Self-assembly of purified recombinant VP1 into capsid-like aggregates[3,4] has shown that switching of the bonding specificity to form the unanticipated[5] non-equivalent connections is an inherent property of the VP1 pentamers. Our map of the inside of the virion displays 72 prongs of electron density extending from the core into the axial cavities of the VP1 pentamers. We identify these prongs with the VP2 and VP3 molecules, which may function to guide the assembly of the highly ordered capsid on the nucleohistone core. The atomic structure of the closely related simian virus-40 capsid has been determined from the high-resolution diffraction data[6]. Our polymavirus map, calculated using all the low-resolution diffraction data, shows no indication of regular order inside the spherical core.

Diffraction data from virion crystals were collected by screened precession photography, in the resolution range 200–22.5-Å spacing, for comparison with previously analysed capsid data[2,7]. Intensities for the three unrecorded lowest order virion reflections and F_{000} were calculated by iterative interpolation using the solvent-flattening restraint[8]. Below 50-Å resolution, there are substantial differences between the virion and capsid data due to diffraction from the inside structure, but at higher resolution the two data sets are similar. To compute a difference map, the two data sets were scaled over the range 0.02–0.044 $Å^{-1}$ by applying an adjustable temperature factor to account for the somewhat greater disorder in the capsid crystals. The capsid preparation[2] consisted predominantly of VP1 with only trace amounts of VP2/VP3. On the approximation that the effective number of scattering electrons in the virion and capsid are proportional to their masses, F_{000} for the virion was scaled to that for the capsid by the ratio of their relative molecular masses. The relative molecular mass (M_r) of an empty capsid, which consists of 360 VP1 molecules[2], is 15.3×10^6. The complete virion[9] includes the minor viral proteins VP2 and VP3 (M_r of 35,000 and 23,000 (35K and 23K) respectively) and the 3,300K circular double-stranded DNA molecule complexes with cellular histones. Data from analyses of the nucleosome[10] and minor protein[11] compositions of the closely related SV40 and polyomavirus[9] indicate that the virion has an M_r of 23,500K ±3%.

Electron-density maps of the virion and capsid (Fig. 1*a*, *b*) were computed at 25-Å resolution from the scaled structure factors and phases that were refined, starting with those previously obtained[2,7] for the capsid structure. The phases for the virion and capsid were subjected to 18 cycles of real space refinement consisting of icosahedral symmetry averaging and solvent flattening outside an envelope whose contour loosely followed the particle surface. For the empty capsid, the envelope was ~10 Å wider than that just enclosing the volume of the 360 VP1 molecules; for the virion, only the outside of this loose envelope was applied in the refinement. The final R factors comparing the transforms of the solvent-flattened, symmetry-averaged virion and capsid maps with the corresponding data were 0.103 and 0.095, respectively. The fluctuations in the difference map (Fig. 1*c*) within the capsid envelope are comparable to the noise level in the solvent volume, which demonstrates the reliability of the phasing and scaling. Because the difference map was calculated using all the low-resolution data and an appropriately scaled F_{000}, the mass distribution of all the inside structure can be quantitatively evaluated.

Surface representations of the virion, capsid and difference maps (Fig. 1*d*–*f*) indicate how the spherical core is connected to the capsid by the 72 prongs. The core is separated from the bases of the pentameric capsomeres by regions of low density (Figs 1*a* and 2), as was observed in the 35-Å-resolution reconstruction of the SV40 virion structure by cryoelectron microscopy[12]. The overall shape and mass distribution of a prong are well defined by the symmetry-averaged difference map (Fig. 2). Scattering matter in the portion of the prong nestled in the VP1 pentamer cavity is packed more densely than near the core, indicating more ordered structure at the tip. Localized density in the same region on the pentamer axis has been found in the high-resolution electron density map of SV40 (ref. 6), which has been identified as a segment of VP2 or VP3.

Evidence for specificity in the interaction between VP1 and the minor capsid proteins implies that the prongs connecting the VP1 pentamers to the core consist of some portion of the VP2/VP3 molecules. Empty capsids, isolated from infected cells, lack detectable nucleohistone but generally contain residual amounts of VP2/VP3, sometimes approaching the normal virion content (W.T.M., unpublished results), indicating a preferential association of the minor proteins with VP1. Furthermore, interaction between recombinant VP1 pentamers and VP3, which requires the carboxyterminal 40-amino-acid segment of VP3, has been demonstrated *in vitro*[13].

The correspondence between the number of prongs (72) and the estimated number of VP2 plus VP3 molecules per virion ($(21+56)\pm10\%$, as evaluated from scaling the SV40 minor protein bands to the VP1 component on SDS-polyacrylamide gels[11]) indicates that each prong represents just one minor protein molecule. VP3 and the C-terminal two thirds of VP2 are coded

† Present address: Enzyme Institute, University of Wisconsin, Madison, Wisconsin 53705, USA.
§ To whom correspondence should be addressed.

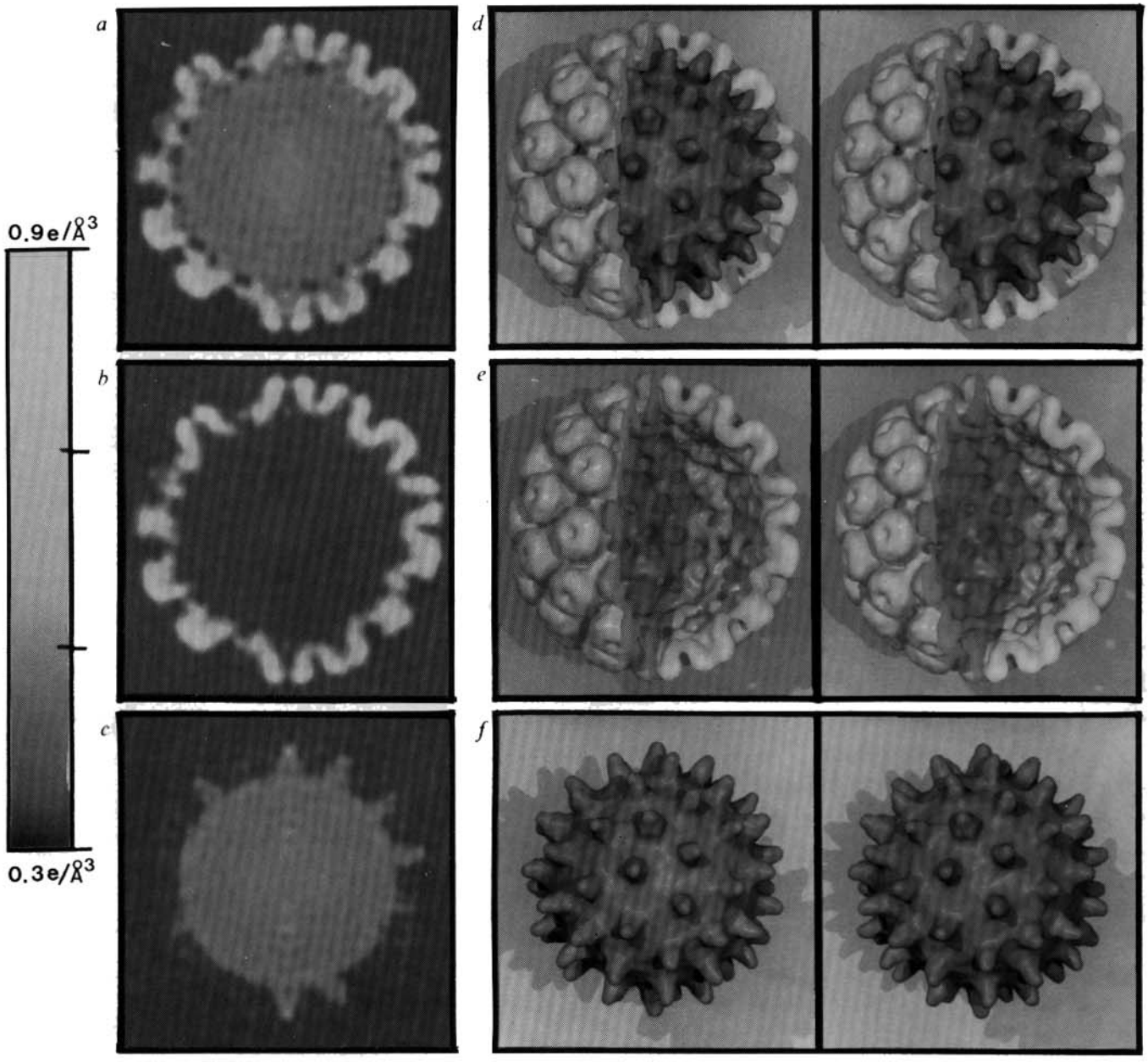

FIG. 1 Sections (*a–c*) and three-dimensional stereographic surface representations (*d–f*) of the electron-density maps of the virion (top), the capsid (middle) and the virion-capsid difference (bottom). The sections *a–c* slice through the centre of the particles and the view is perpendicular to both an icosahedral 5-fold axis (running vertically) and a local hexavalent pentamer axis (22° to the right of the icosahedral 5-fold axis at the upper part of the sections). The outer diameter of the capsid measured along a 5-fold axis is 500 Å. The grey scale to the left defines the electron density levels in the maps. Sections *a–c* are from the icosahedrally averaged maps computed using the measured structure factors with the refined phases. The three-dimensional surface display of the capsid map (*e*) was contoured to contain a volume equal to that calculated from the mass and partial specific volume of the 360 VP1 molecules. In *d* and *e*, a 108° sector was removed from the VP1 capsid structure, such that the cut surface is equivalent to the section of the capsid in *a* and *b*. The surface contour for the difference map (*f*) was set such that the prongs projecting from the core nestled inside the axial cavities of the VP1 pentamers in the virion map (*d*).

by the same DNA sequence[9]. Deletion mutants of SV40 lacking VP2 were found to reproduce slowly, but viable mutants without VP3 were not detected[14]. Thus, the N-terminal third of VP2 is not required for viral assembly, but some portion of the VP3 sequence seems to be essential. We conclude that the prongs comprise the part of VP3 or the equivalent part of VP2 involved in connecting the VP1 pentamers to the nucleohistone core.

How much protein is in the connecting prongs has been estimated by integration of the electron density distribution in our difference map (Figs 1*c* and 2). In the hexavalent and pentavalent positions, the mass-per-prong domain (as delineated in Fig. 2) is 14.8K and 18.9K, respectively, but the difference in these values is within the uncertainty of the measurements. The mean mass of a 50-Å-long prong domain (15.5K) accounts for about two thirds of a VP3 molecule. Although electron density carries no chemical label, the correlation of biochemical and structural data indicates that the prong domain corresponds to a major portion of the VP3 sequence. Similarly, identification of the spherical core with an irregular packing of the ~26 nucleosomes of the minichromosome is consistent with data on the nucleohistone structure[9,10,15].

The core density distribution appears spherically symmetric

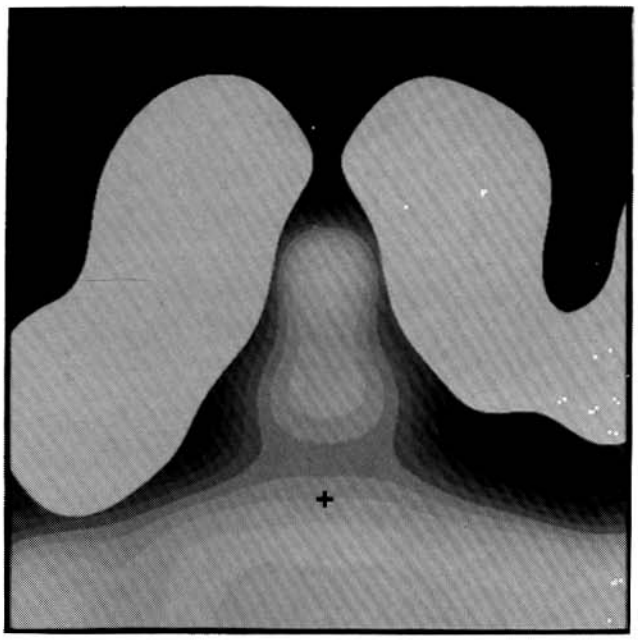

FIG. 2 Section of the symmetry-averaged difference map of a prong inserted in the outline of a VP1 capsomere. Five sections related by the local hexavalent pentamer axis and one corresponding section of a pentavalent pentamer (oriented as in Fig. 1*c*) were averaged to generate this map. The section of the prong map, displayed on a 12-step grey scale, is contained inside the outline of the capsid envelope as contoured in Fig. 1*e*. The step interval of the grey scale is 0.0065 electrons/Å^3, which corresponds to the r.m.s. noise level measured from the fluctuations in the solvent volume of the electron-density map. The figure frame is 120-Å square and the pentamer axis is vertical at the middle. The plus sign marks the level defined as the boundary between the core and the prong, which is at radii of 174 and 170 Å on the pentavalent and hexavalent pentamer axes, respectively.

within the noise level measured from the solvent portions of the maps (Fig. 1*a*–*c*). At the centre, the core density is higher than near its surface, as shown by the spherically averaged density profiles (Fig. 3). The measured density distribution can be accounted for by about four nucleosomes that occupy the centre of the core out to ~85 Å radius, and a mean of ~22 nucleosomes, less compactly packed, in the shell from ~85–170 Å radius. Although there is no evidence of any icosahedral order within the core, there must be some type of local order among the closely packed nucleosomes which varies from virion to virion in the crystals. The liquid-drop model for the isolated compact minichromosome, inferred from cryoelectron microscopy[15], may also represent the irregular packing of the nucleosomes in the virion.

Capsid proteins of the DNA tumour viruses are synthesized in the host cell cytoplasm and are then transported to the nucleus where they assemble with the viral minichromosomes to form the icosahedral virus particles[9]. VP1 molecules expressed in insect cells are also transported to the nucleus where the pentamers self-assemble into capsids independently of the minor capsid proteins and minichromosome[16]. In normally infected cells, association of VP1 pentamers with the common C-terminal portion of VP2 or VP3 can occur in the cytoplasm[13] or in the nucleus, because both VP1 and the minor protein have their own nuclear targeting sequences[17]. Insertion of only a single minor protein segment in the pentagonally symmetric cavity can be accounted for by the steric restraints. The extended N-terminal third of VP2, which is not required for viral assembly[14], may form a flexible arm holding the terminal myristyl group, which seems to enhance the efficiency of viral entry into the host cell[18]. The essential function of VP3 and the corresponding part of VP2 is apparently to direct the self-assembly of VP1 pentamers on the nucleohistone core, thereby insuring formation of the complete virion. □

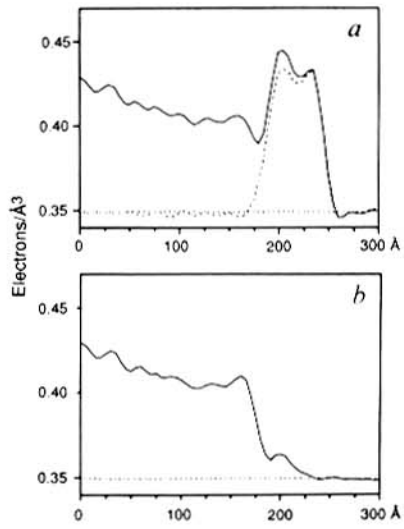

FIG. 3 Spherically averaged electron-density profiles of *a*, the capsid (dashed curve) and virion (solid curve) and *b*, the difference between them. These spherical averages were computed from the three-dimensional maps, which were scaled according to the effective number of scattering electrons per unit cell, with the solvent density of 0.35 electrons Å^{-3}. The virion and capsid profiles superimpose from about 226 to 250 Å radius. From 0–226 Å radius, the difference (*b*) between the virion and capsid profiles maps the radial distribution of the matter inside the virion. The virion profile shows a region of low density at around 175-Å radius, which indicates the boundary between the core and the bases of the capsomeres. The ripples in the core region of the profiles are the order of the noise fluctuations in the spherically averaged density measurements.

Received 28 October; accepted 12 December 1991.

1. Adolph, K. W. *et al. Science* **203,** 1117–1119 (1979).
2. Rayment, I., Baker, T. S., Caspar, D. L. D. & Murakami, W. T. *Nature* **295,** 110–115 (1982).
3. Salunke, D. M., Caspar, D. L. D. & Garcea, R. L. *Cell* **46,** 895–904 (1986).
4. Salunke, D. M., Caspar, D. L. D. & Garcea, R. L. *Biophys. J.* **56,** 887–900 (1989).
5. Caspar, D. L. D. & Klug, A. *Cold Spring Harb. Symp. quant. Biol.* **27,** 1–24 (1962).
6. Liddington, R. C. *et al. Nature* **354,** 278–284 (1991).
7. Rayment, I., Baker, T. S. & Caspar, D. L. D. *Acta crystallogr.* B**39,** 505–516 (1983).
8. Rayment, I. *Acta crystallogr.* A**39,** 102–116 (1983).
9. Tooze, J. (ed.) *DNA Tumor Viruses* Part 2, 2nd ed (Cold Spring Harbor Laboratory, New York, 1981).
10. Ambrose, C., McLaughlin, R. & Bina, M. *Nucleic Acids Res.* **15,** 3703–3721 (1987).
11. Lin, W., Hata, T. & Kasamatsu, H. *J. Virol.* **50,** 363–371 (1984).
12. Baker, T. S., Drak, J. & Bina, M. *Proc. natn. Acad. Sci. U.S.A.* **85,** 422–426 (1988).
13. Gharakhanian, E., Takahashi, J., Clever, J. & Kasamatsu, H. *Proc. natn. Acad. Sci. U.S.A.* **85,** 6607–6611 (1988).
14. Cole, C. N., Landers, T., Goff, S. P., Manteuil-Brutlag, S. & Berg, P. *J. Virol.* **24,** 277–294 (1977).
15. Dubochet, J., Adrian, M., Schultz, P. & Oudet, P. *EMBO J.* **5,** 519–528 (1986).
16. Montross, L. *et al. J. Virol.* **65,** 4991–4998 (1991).
17. Clever, J. & Kasamatsu, H. *Virology* **181,** 78–90 (1991).
18. Krauzewicz, N. *et al. J. Virol.* **64,** 4414–4420 (1990).

ACKNOWLEDGEMENTS. We thank R. L. Garcea, S. C. Harrison and J. Badger for advice and information. This work was supported by a US Public Health Service grant from the National Cancer Institute (D.L.D.C.) and an American Cancer Society grant (W.T.M.).